

# Percolation and Magnetization for Generalized Continuous Spin Models

Santo Fortunato and Helmut Satz

Fakultät für Physik, Universität Bielefeld  
D-33501 Bielefeld, Germany

## Abstract:

For the Ising model, the spin magnetization transition is equivalent to the percolation transition of Fortuin-Kasteleyn clusters. This result remains valid also for the continuous spin Ising model. We show on the basis of numerical simulations that such an equivalence can be generalized to a wider class of theories, including spin distribution functions, longer range interactions and self-interaction terms.

## Introduction

Percolation theory [1, 2] has been successfully applied to describe continuous thermal phase transitions as geometrical transitions: at the critical threshold, suitably defined clusters becomes infinite (see [3] - [6]). It is moreover possible to establish a correspondence between thermal and cluster variables, such that the critical exponents of corresponding variables coincide [4]. This provides an intuitive geometric description of the mechanism of the thermal transition; e.g., in the case of the Ising model, we can identify clusters as magnetic domains, so that magnetization sets in when they span the lattice. In a recent study [7], we have tried to extend this picture to the confinement-deconfinement transition of  $SU(2)$  gauge theory. This theory leads to a continuous phase transition which belongs to the universality class of the Ising model, due to the common  $Z(2)$  global symmetry of the corresponding Hamiltonians [8]. However, our result is valid only in the strong coupling limit of  $SU(2)$ , where the partition function can be well approximated [9] by that of a continuous spin Ising model. In this model, the correspondence between percolation and thermal variables can be rigorously established [10]. For a general study of  $SU(2)$  gauge theory, the weak coupling limit must be taken into account, and there the approximations used in [9] are no longer valid.

To address the deconfinement problem more generally, it may be helpful to look for an effective theory for  $SU(2)$ . An interesting attempt in this direction was proposed some time ago in the search for the fixed point of the theory by means of block-spin transformations [11]. There the original Polyakov loop configurations were projected onto configurations of Ising-like spins according to the sign of the Polyakov loop at each lattice site. This assumes that for the criticality only the global  $Z_2$  symmetry of the theory is important. As a result of this projection one obtains an effective Hamiltonian with only short-range couplings, although some of the resulting couplings correspond to interactions beyond the fundamental nearest-neighbour form. Moreover, the assumption that only the  $Z_2$  symmetry of the theory is relevant must be tested.

In this paper we want to study through numerical simulations if in continuous spin models the introduction of non-uniform spin distributions, or the introduction of additional longer range interactions, still allows a description of the thermal transition in terms of percolation. Such extensions would seem necessary prerequisites for a general percolation formulation of  $SU(2)$ . We will first show that the presence of spin distribution functions does not affect the equivalence of thermal and percolation transitions, provided we define clusters through bonds established by a probability of Fortuin-Casteleyn form between like-sign spins. Subsequently we turn to longer range interactions and to the inclusion of self-interaction terms and show that also here the equivalence remains valid.

Our study is based on continuous spin Ising models, in which the individual spins  $s_i$  at each lattice site can take on all values in the finite range  $[-1, 1]$ , with the distribution of the spins governed by a spin distribution function  $f(s_i)$ . For  $f(s) = \delta(|s| - 1) \forall i$  and only nearest-neighbour (NN) interactions, we recover the conventional Ising model. For  $f(s_i) = 1 \forall i$  and only NN interactions, we obtain the continuous spin model studied in [10]. Here we will consider four more general models of this type;  $d$  denotes the space dimension:

- A)  $d = 2$ , only NN interactions, but a non-uniform spin distribution  $f(s_i)$ ;
- B)  $d = 2$ ,  $f(s_i) = 1 \forall i$ , NN and diagonal next-nearest-neighbour (NTN) interaction (Fig. 1);
- C)  $d = 3$ ,  $f(s_i) = 1 \forall i$ , NN and two types of NTN interactions (see Fig. 2);
- D) as case C), but including an additional self-interaction term proportional to  $s_i^2 \forall i$ .

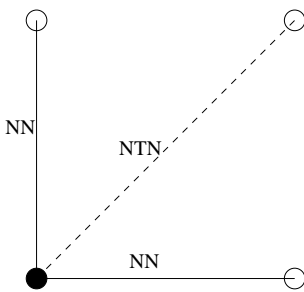


Figure 1. Spin interactions in model B.

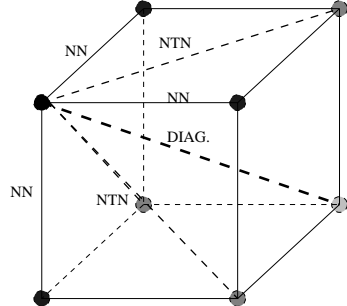


Figure 2. Spin interactions in model C.

In all four cases, the equivalence of thermal and percolation critical behaviour will be addressed by calculating the transition points, the critical exponents, and the rescaling behaviour of quantities corresponding to Binder cumulants.

## Model A: Spin Distribution Function

The spin variable  $s$  can take all values in  $[-1, 1]$ . It is convenient to rewrite it in the form

$$s = \text{sign}(s)\sigma, \quad (1)$$

separating the sign from the amplitude of the spin. Since we want to retain the Z(2) symmetry of the Hamiltonian, the signs of the spins are equidistributed. In contrast, the amplitudes can in general be weighted in different ways by choosing a distribution function  $f(\sigma)$ . The partition function of such a model then has the form

$$Z(T) = \prod_i \int_0^1 d\sigma_i f(\sigma_i) \exp\{\kappa \sum_{\langle i,j \rangle} s_i s_j\}, \quad (2)$$

where  $\kappa \equiv J/T$ , with  $J$  denoting the spin coupling energy and  $T$  the temperature. Since we want to study models with continuous transitions, the choice of the function  $f(\sigma)$  is not arbitrary. It can be proved that it must obey certain regularity conditions, which are not very restrictive, however [12]. In [10], the amplitudes were equidistributed, with  $f(\sigma) = 1$ . Here we consider the following form for  $f(\sigma)$ :

$$f(\sigma) = \sqrt{1 - \sigma^2} \quad (3)$$

which is the Haar measure of the SU(2) group; it appears in the strong coupling approximation of SU(2) [9]. To define a cluster, we use exactly the same procedure as in [10], i.e., we join nearest-neighbouring spins of the same sign with the bond probability  $p = 1 - \exp(-2\kappa\sigma_i\sigma_j)$ , where  $\sigma_i$  and  $\sigma_j$  are the amplitudes of the two spins. We use free boundary conditions and define percolation when a cluster spans the lattice in each of the two directions. This is done to exclude the possibility that, due to the finite size of our lattices, one could find more than one percolation cluster, which would make the definition of our variables ambiguous. We shall use this definition for all the models to be considered here<sup>1</sup>.

The percolation variables to be studied are: the *percolation strength*  $P$ ,

$$P = \frac{\text{size of the percolating cluster}}{\text{volume of the lattice}}. \quad (4)$$

and the *average cluster size*  $S$ ,

$$S = \sum_s \left( \frac{n_s s^2}{\sum_s n_s s} \right). \quad (5)$$

Here  $n_s$  is the number of clusters of size  $s$  and the sums exclude the percolating cluster. Besides these two, we evaluate another very useful variable. For a given lattice size and a value of  $\kappa$ , we determine the relative fraction of configurations containing a percolating cluster. This *percolation probability*  $\gamma_r(\kappa)$  is a scaling function, analogous to the Binder cumulant  $g_r(\kappa)$  [13].

---

<sup>1</sup>In three dimensions even this definition of a spanning cluster does not exclude the possibility of having more than one such cluster in the same configuration. Nevertheless the occurrence of these cases is so small that we can safely ignore them.

In addition to these percolation variables, we also measure the lattice averages of energy and magnetization, in order to study the thermal transition as well. From the magnetization  $M$  we calculate in particular the physical susceptibility  $\chi$ ,

$$\chi(\kappa) = V (\langle M^2 \rangle - \langle M \rangle^2) \quad (6)$$

and the Binder cumulant  $g_r$ ,

$$g_r(\kappa) = \frac{\langle M^4 \rangle}{\langle M^2 \rangle^2} - 3 . \quad (7)$$

We have performed simulations on four lattice sizes, from  $64^2$  to  $240^2$ . Our algorithm consists in heatbath steps for the update of the spin amplitudes followed by Wolff-like cluster updates for the flipping of the signs. That is basically the same method as used in [10], although the heatbath procedure is slightly modified to take into account the presence of the distribution function  $f(\sigma)$ . The proof that the detailed balance condition is satisfied for such a cluster update is obtained following the derivations in [14] - [17]. Flipping the spins reduces drastically the autocorrelation time, which allowed us to collect extensive data and thus reduce the errors.

Figure 3 shows a comparison between the thermal variable  $g_r(\kappa)$  and the percolation probability  $\gamma_r(\kappa)$ , both as functions of the temperature variable  $\kappa$ , for different lattice sizes. The points where the lines cross are the infinite volume thresholds for the thermal and the geometrical transition, respectively. The agreement between the two points is remarkable.

Since the percolation probability is a scaling function, we can already get an indication about the critical exponents of the percolation transition. Given the critical point and the exponent  $\nu$ , a rescaling of the percolation probability as a function of  $(\kappa - \kappa_{cr})L^{1/\nu}$  should give us the same function for each lattice size ( $L$  is the linear dimension of the lattice). Figs. 4 and 5 show the rescaled percolation probability, using  $\kappa_{cr} = 1.3888$  with the random percolation exponent  $\nu = 4/3$  and Ising exponent  $\nu = 1$ , respectively. The figures clearly show scaling for the Ising exponent and no scaling for the random percolation exponent.

The exponent  $\beta$  governs percolation strength and magnetization, while  $\gamma$  governs cluster size and susceptibility. To determine them, we have performed high-statistics simulations around the critical point, with the number of measurements for each value of the coupling varying from 50000 to 100000. We have then used the  $\chi^2$  method [18] to determine the values of the exponents. The results are shown in Table I, where the first row shows the calculated percolation results, the second the corresponding magnetization calculations, and the third the analytically known Ising model values. It is evident that the percolation behaviour coincides fully with the thermal critical behaviour. This conclusion is likely to hold in general for the admissible spin distribution functions, and it should be possible to prove it rigorously following the method used in [20].

## Model B: Next-to-Nearest Neighbour Interactions

We now want to study how to correctly define clusters in the presence of more than the standard nearest-neighbour interactions. We have now two terms, with a Hamiltonian

of the form

$$\mathcal{H} = J_{NN} \sum_{\langle i,j \rangle}^{NN} s_i s_j + J_{NTN} \sum_{\langle i,j \rangle}^{NTN} s_i s_j \quad (8)$$

where the first sum describes nearest-neighbour and the second diagonal next-to-nearest neighbour interactions (Fig. 1). Since longer range interactions are generally weaker, we have fixed the ratio between the two couplings at  $J_{NN}/J_{NTN} = 10$ ; however, we do not believe that our results depend on the choice of the couplings, as long as both are ferromagnetic. To define clusters, we now extend the Coniglio-Klein method and define for each two spins  $i, j$  of the same sign, for NN as well as NTN, a bond probability

$$p_B^x = 1 - \exp\{-2\kappa_x \sigma_i \sigma_j\}, \quad (9)$$

where  $x$  specifies  $\kappa_{NN} = J_{NN}/T$  and  $\kappa_{NTN} = J_{NTN}/T$ , respectively. This hypothesis seems to us the most natural, and we will test it in the following models B, C, and D. models. We recall that in model B, as well as in C and D, we assume a spin equidistribution, i.e.,  $f(\sigma) = 1$ .

We have studied model B using two different Monte Carlo algorithms, in order to test if a Wolff-type algorithm can also be applied in the presence of NTN interactions. The first is the standard Metropolis update, while the second alternates heat bath steps and a generalized Wolff flipping, for which the clusters are formed taking into account both interactions. The generalization of the cluster update is trivial. After several runs, some with high statistics, we found excellent agreement with the Metropolis results in all cases. So, the mixed algorithm with heat bath and Wolff flippings appears to remain viable also in the presence of more than the standard NN interaction. Subsequently we have therefore used this mixed algorithm. The lattice sizes for model B ranged from  $100^2$  to  $400^2$ .

As for model A, we now show for model B the comparison between percolation probability and Binder cumulant, in order to test that the critical points coincide (Fig. 6). We then again rescale the percolation probability, using the critical  $\kappa$  determined in Fig. 6 together with the exponent  $\nu$  from the  $d = 2$  random percolation transition ( $\nu = 4/3$ ) and the  $d = 2$  Ising model ( $\nu = 1$ ). Figs. 7 and 8 indicate that again the correct exponent is that of the Ising model.

The determination of the other two exponents  $\beta$  and  $\gamma$  by means of the  $\chi^2$  method confirms that indeed the exponents of our geometrical islands belong to the Ising universality class (Table II).

### Model C: Extension to Three Dimensions

To extend the results found in Model B for two dimensions, we have repeated the study for a  $d = 3$  model with three different interactions (Figure 2). To fix the model, we have to specify the ratios of the nearest-neighbour coupling  $\kappa_{NN}$  to  $\kappa_{NTN}$  and  $\kappa_{diag}$ . We chose them to be 10:2 and 10:1, respectively. Our  $d = 3$  calculations are performed on lattices ranging from  $12^3$  to  $40^3$ .

Also here we have first compared the results from a mixed algorithm of the same kind as for the previous case to those from a standard Metropolis algorithm; again, the agreement is very good. Figs. 9, 10 and 11 then show the comparison of the thresholds

and the scaling of the percolation probability. As before, the correspondence between percolation and thermal variables is evident (Table III).

### Model D: Adding Self-Interaction

From what we have seen up to now, it seems to be clear that the correct cluster definition can readily be extended to models including several (ferromagnetic) spin-spin interactions. However, such terms are not the only possible interactions in a model with  $Z(2)$  symmetry and a continuous transition. There could be anti-ferromagnetic spin-spin couplings as well as multispin terms, coupling an even number of spins greater than two (four, six, etc.). Moreover, since the spins are continuous, the presence of self-interaction terms is possible, determined by  $s^2$ ,  $s^4$ , etc. The treatment for antiferromagnetic and multispin couplings so far remains an open question. In contrast, self-interactions are not expected to play a role in the cluster building, since such terms do not relate different spins. Therefore, we test a cluster definition ignoring any self-interaction term.

We thus consider in Model D the same interactions as in Model C, plus a term proportional to  $J_0 \sum_i s_i^2$ . We chose a negative value for the self-interaction coupling  $J_0$ ; this is the more interesting case since the corresponding interaction tries to resist the approach of the system to the ground state at low temperatures ( $\sigma = 1$  everywhere). The ratios of the NN coupling to the others were chosen as  $J_{NN} : J_{NTN} : J_{diag} : J_0 = 6 : 2 : 1 : 2$ .

Again we first verify the viability of the mixed algorithm and then determine the rescaled percolation probability (Fig. 12) and the critical exponents (Table IV). It is evident that percolation and the thermal transition again fall into the same universality class.

## Conclusions

We have shown that the equivalence of cluster percolation and spin ordering in the description of critical behaviour in the continuous spin Ising model can be extended to a rather wide class of theories. In particular, it remains valid also in the presence of more than just nearest neighbour interactions and of spin distribution functions. Moreover, the introduction of self-energy contributions does not affect the equivalence. All these features will enter in the further extension to  $SU(2)$  gauge theories, and the fact that they do not interfere with a percolation formulation of critical behaviour provides support for such efforts.

## Acknowledgements

It is a pleasure to thank D. Gandolfo for helpful discussions. We would also like to thank the TMR network ERBFMRX-CT-970122 and the DFG Forschergruppe Ka 1198/4-1 for financial support.

## References

[1] D. Stauffer and A. Aharony, *Introduction to Percolation Theory*, Taylor & Francis, London 1994.

- [2] G. Grimmett, *Percolation*, Springer-Verlag, 1999.
- [3] M. E. Fisher, Physics **3**, 255-283 (1967).
- [4] A. Coniglio and W. Klein, J. Phys. A. **13**, 2775 (1980).
- [5] L. Chayes, Comm. Math. Phys. **197**, 623 (1998).
- [6] M. Campbell and L. Chayes, J. Phys. A. **31**, L255-L259 (1998).
- [7] S. Fortunato and H. Satz, Phys. Lett. B **475**, 311-314 (2000).
- [8] B. Svetitsky and L. G. Yaffe, Nucl. Phys. B **210**, 423 (1982).
- [9] F. Green and F. Karsch, Nucl. Phys. B **238**, 297 (1984).
- [10] P. Bialas et al, hep-lat/9911020, Nucl. Phys. B (in press).
- [11] M. Okawa, Phys. Rev. Lett. **60**, 1805-1808 (1988).
- [12] R. S. Ellis, J. L. Monroe, C. M. Newman, Comm. Math. Phys. **46**, 167-182 (1976).
- [13] K. Binder and D. W. Heermann, *Monte Carlo simulations in Statistical Physics*, Springer-Verlag 1988.
- [14] U. Wolff, Nucl. Phys. B **322**, 759 (1989).
- [15] T. E. Harris, Proc. Camb. Phil. Soc. **56**, 13 (1960).
- [16] L. Chayes and J. Machta, Physica A **329**, 542 (1997).
- [17] L. Chayes and J. Machta, Physica A **254**, 477 (1998).
- [18] J. Engels et al., Phys. Lett. B **365**, 219 (1996).
- [19] A. M. Ferrenberg and D. P. Landau, Phys. Rev. B **44**, 5081 (1991).
- [20] Ph. Blanchard, L. Chayes, D. Gandolfo, submitted to J. Stat. Phys.

	$\kappa_{cr}$	$\beta/\nu$	$\gamma/\nu$	$\nu$
Percolation	$1.3887^{+0.0002}_{-0.0001}$	$0.128^{+0.007}_{-0.010}$	$1.754^{+0.007}_{-0.008}$	$0.99^{+0.03}_{-0.02}$
Magnetization	$1.3888^{+0.0002}_{-0.0003}$	$0.121^{+0.008}_{-0.006}$	$1.745^{+0.011}_{-0.007}$	$1.01^{+0.02}_{-0.03}$
Ising Model		$1/8$	$7/4$	1

Table I. Thermal and percolation thresholds and exponents of Model A.

	$\kappa_{cr}$	$\beta/\nu$	$\gamma/\nu$	$\nu$
Percolation	$0.9708^{+0.0002}_{-0.0002}$	$0.129^{+0.008}_{-0.009}$	$1.752^{+0.009}_{-0.011}$	$1.005^{+0.012}_{-0.020}$
Magnetization	$0.9707^{+0.0003}_{-0.0002}$	$0.124^{+0.007}_{-0.005}$	$1.747^{+0.009}_{-0.007}$	$0.993^{+0.014}_{-0.010}$
Ising Model		$1/8$	$7/4$	1

Table II. Thermal and percolation thresholds and exponents of Model B.

	$\kappa_{cr}$	$\beta/\nu$	$\gamma/\nu$	$\nu$
Percolation	$0.36673^{+0.00012}_{-0.00010}$	$0.528^{+0.012}_{-0.015}$	$1.9850^{+0.010}_{-0.015}$	$0.632^{+0.01}_{-0.015}$
Magnetization	$0.36677^{+0.00010}_{-0.00008}$	$0.530^{+0.012}_{-0.018}$	$1.943^{+0.019}_{-0.008}$	$0.640^{+0.012}_{-0.018}$
Ising Model [19]		$0.518^{+0.007}_{-0.007}$	$1.970^{+0.011}_{-0.011}$	$0.6289^{+0.0008}_{-0.0008}$

Table III. Thermal and percolation thresholds and exponents of Model C.

	$\kappa_{cr}$	$\beta/\nu$	$\gamma/\nu$	$\nu$
Percolation	$0.3005^{+0.0001}_{-0.0001}$	$0.524^{+0.010}_{-0.011}$	$1.9750^{+0.008}_{-0.009}$	$0.636^{+0.011}_{-0.017}$
Magnetization	$0.3004^{+0.0002}_{-0.0001}$	$0.513^{+0.012}_{-0.010}$	$1.963^{+0.014}_{-0.009}$	$0.626^{+0.011}_{-0.010}$
Ising Model [19]		$0.518^{+0.007}_{-0.007}$	$1.970^{+0.011}_{-0.011}$	$0.6289^{+0.0008}_{-0.0008}$

Table IV. Thermal and percolation thresholds and exponents of Model D.

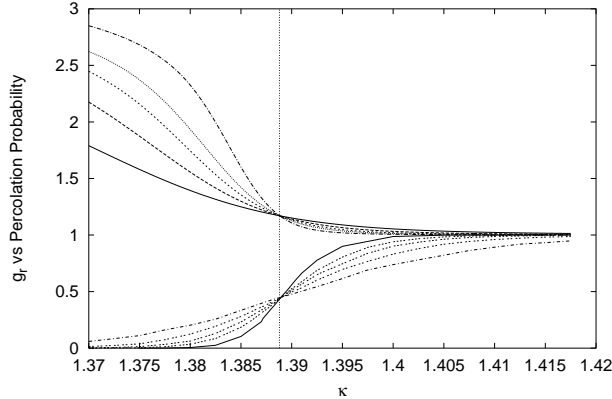


Figure 3. Comparison of the thermal and the geometrical critical point for Model A obtained respectively from the Binder cumulant  $g_r$  and the percolation probability.

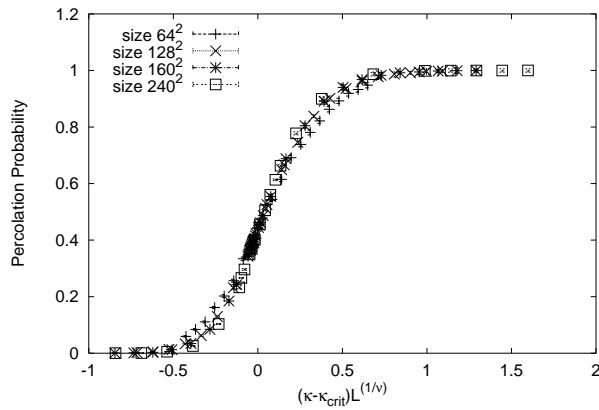


Figure 4. Rescaled percolation probabilities for Model A using the 2-dimensional random percolation exponent  $\nu = 4/3$ .

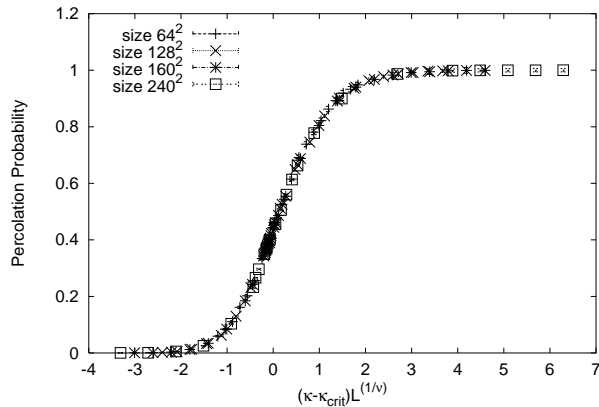


Figure 5. Rescaled percolation probabilities for Model A using the 2-dimensional Ising exponent  $\nu = 1$ .

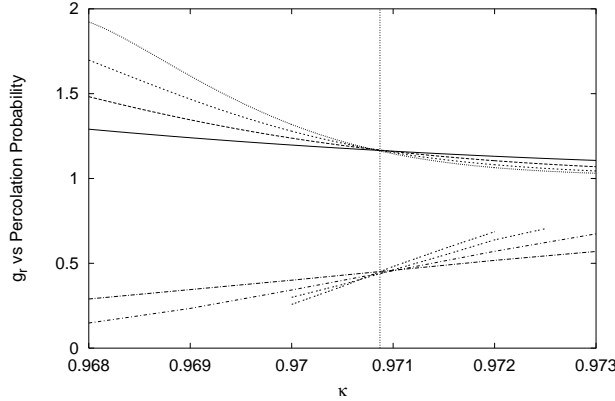


Figure 6. Comparison of the thermal and the geometrical critical point for Model B obtained respectively from the Binder cumulant  $g_r$  and the percolation probability.

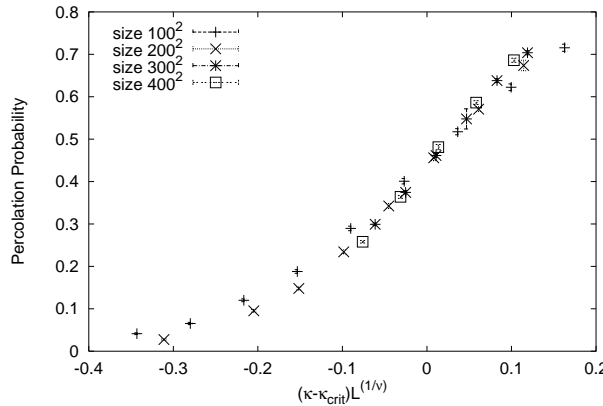


Figure 7. Rescaled percolation probabilities for Model B using the 2-dimensional random percolation exponent  $\nu = 4/3$ .

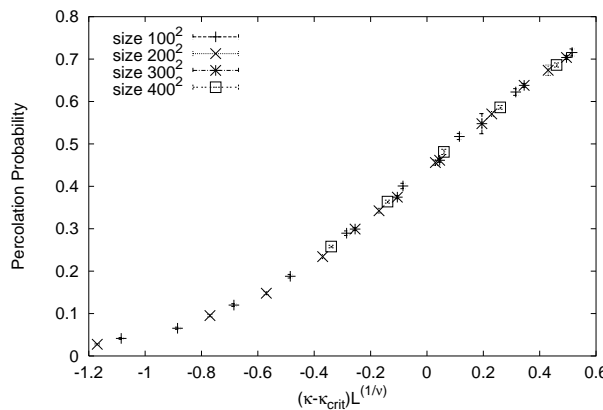


Figure 8. Rescaled percolation probabilities for Model B using the 2-dimensional Ising exponent  $\nu = 1$ .

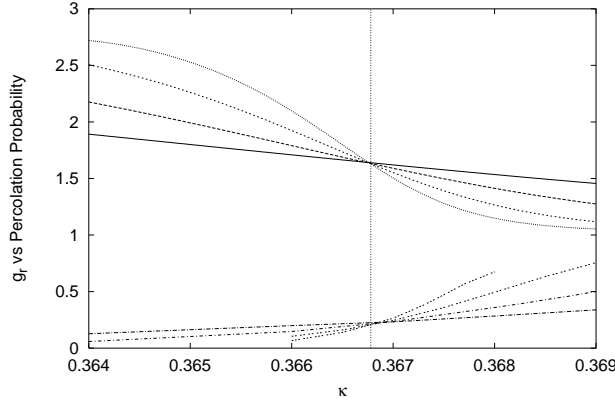


Figure 9. Comparison of the thermal and the geometrical critical point for Model C obtained respectively from the Binder cumulant  $g_r$  and the percolation probability.

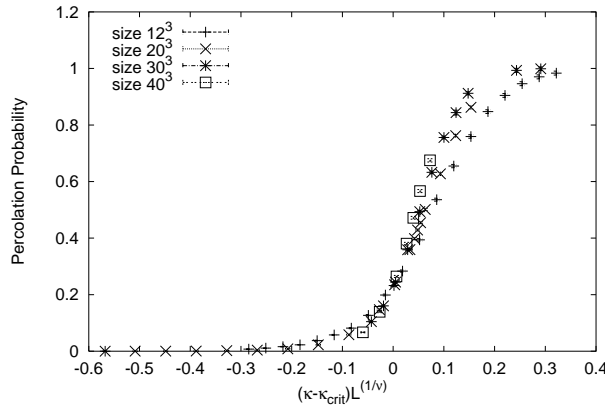


Figure 10. Rescaled percolation probabilities for Model C using the 3-dimensional random percolation exponent  $\nu = 0.88$ .

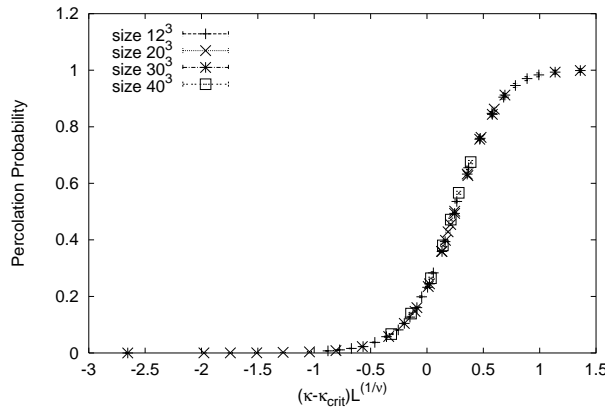


Figure 11. Rescaled percolation probabilities for Model C using the 3-dimensional Ising exponent  $\nu = 0.629$ .

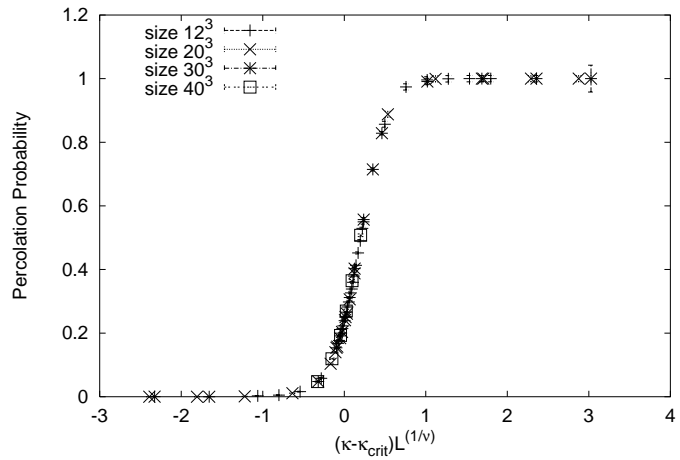


Figure 12. Rescaled percolation probabilities for Model D using the 3-dimensional Ising exponent  $\nu = 0.629$ .

